Supplementary Information

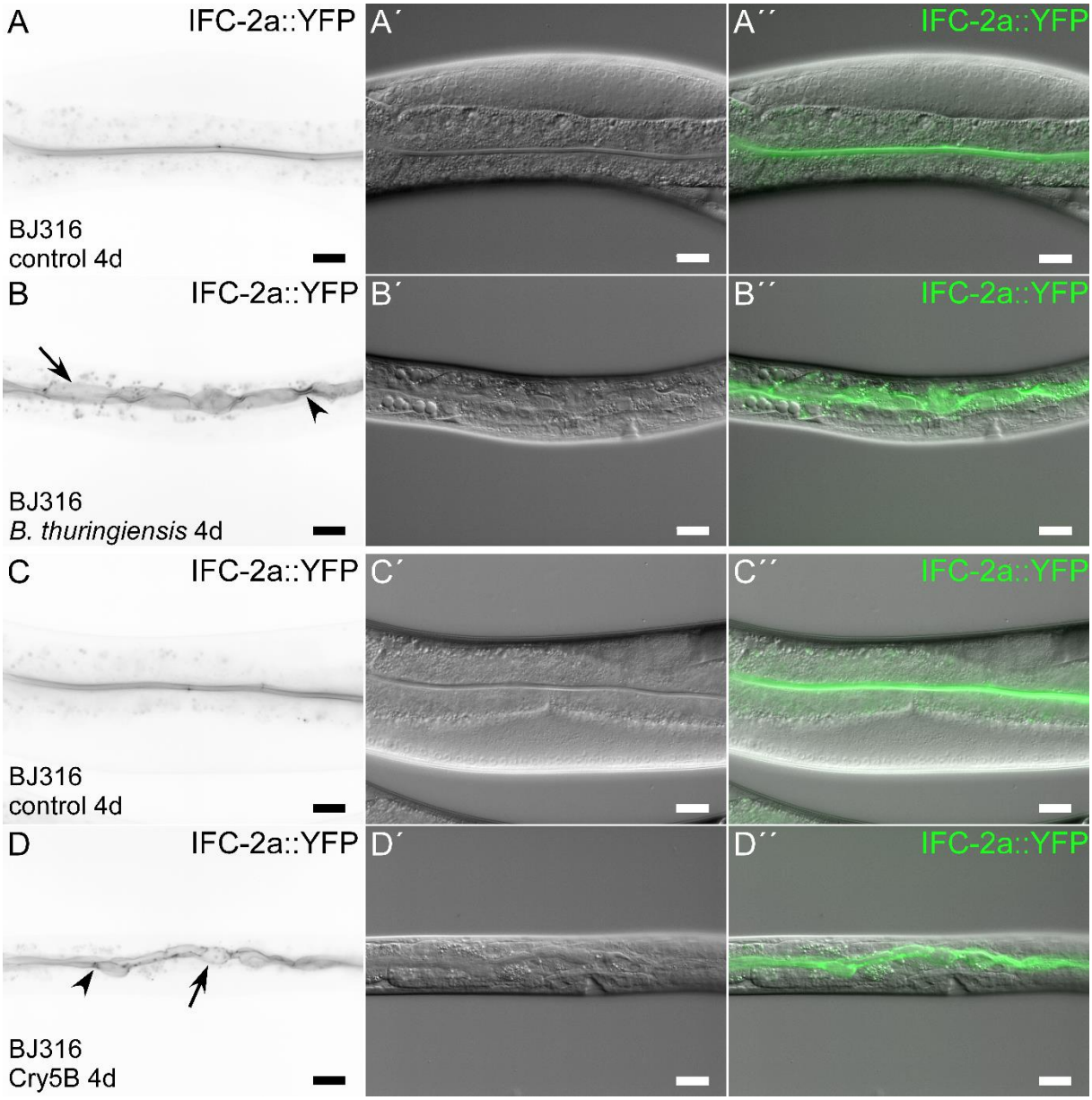

Fig. S1. IFC-2a::YFP redistributes upon infection with *Bacillus thuringiensis* or intoxication with Cry5B. The *in vivo* images show the distribution of the fluorescent IF protein IFC-2a::YFP that is produced from a *yfp*-tagged version of the endogenous *ifc-2a* gene (A-D; corresponding interference contrast images in A'-D'; merged images in A''-D''). Animals were grown for 4 days after hatching on OP50 (A-A''), *Bacillus thuringiensis* DB27 (B-B''), empty vector-containing control JM103 (C-C''), and Cry5B pore-forming toxin-producing JM103 (D-D''). Animals grown on control bacteria (OP50, control JM103) reach adulthood and display smooth periluminal localization of IFC-2a::YFP in the intestine (A-A'', C-C'') indistinguishable

from IFB-2a::CFP (Fig. 1C-C'', E-E'') indicating an intact intestinal lumen surrounded by a fully developed endotube. In contrast, infection with *Bacillus thuringiensis* DB27 (B-B'') or intoxication with its pore-forming toxin Cry5B (D-D'') induce intestinal lumen dilation and multiple cytoplasmic invaginations of the IF-rich endotube as also seen in the IFB-2a::CFP reporter strain (see Fig. 1D-D'', F-F''). Scale bars: 20 μm in A-D''.

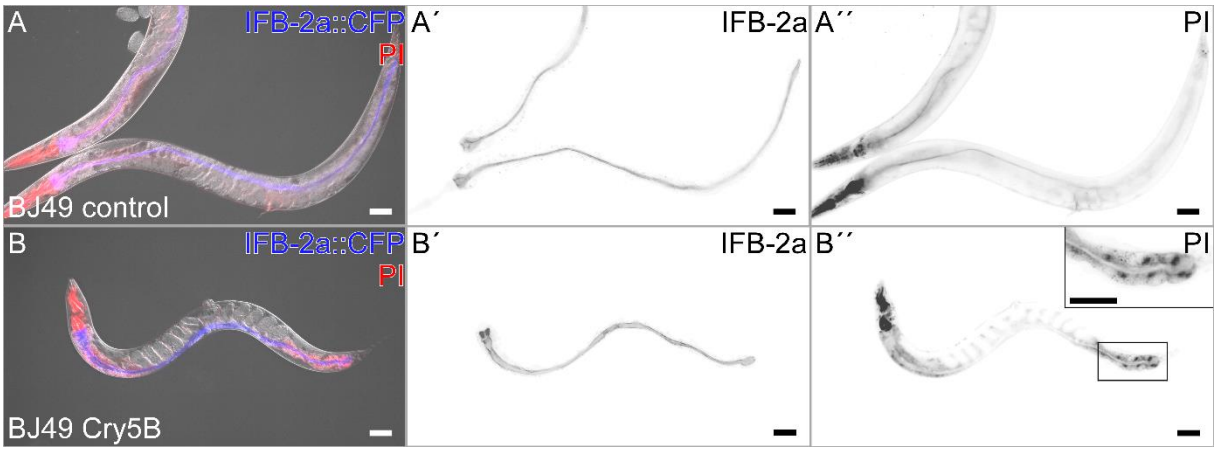

Fig. S2. The pore-forming toxin Cry5B induces pores at the apical plasma membrane of the intestinal cells without affecting junctional tightness. IFB-2a::CFP-producing reporter strain was first incubated either on control or on Cry5B-expressing JM103 for 24 hours. Animals were subsequently fed with the fluorescent tracer propidium iodide for 2 hours to assess intestinal integrity. The micrographs show that propidium iodide is retained in the intestinal lumen surrounded by a characteristic IFB-2a-positive endotube in the control (A-A'') but enters intestinal nuclei after Cry5B treatment, which has only elicited minor alterations in IFB-2a distribution at this time point (B-B''). Note that intercellular uptake of propidium iodide is not detectable indicating that the *C. elegans* apical junction is not affected by Cry5B intoxication. The uterine propidium iodide fluorescence in (A'' and B'') is caused by tracer uptake through the vulva. Scale bars: 50 µm.

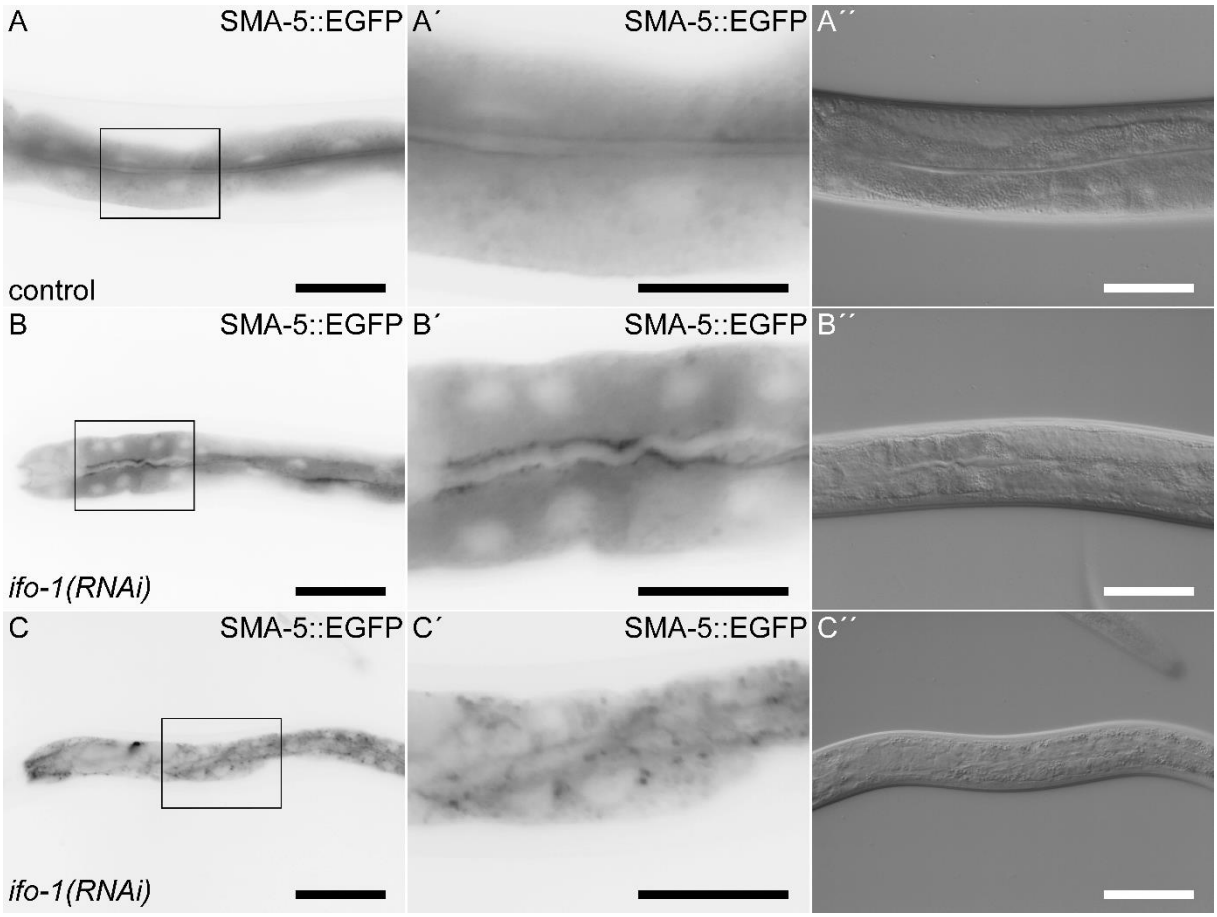

Fig. S3. SMA-5 accumulates apically and in cytoplasmic dots in *ifo-1(RNAi)* animals. The images (fluorescence micrographs in A-C with enlargements of boxed areas in A'-C' and corresponding interference contrasts in A''-C'') show that SMA-5::EGFP is uniformly localized in the intestinal cytoplasm and the apical plasma membrane of control animals (A-A'') but accumulates apically and in cytoplasmic dots in *ifo-1(RNAi)* intestines (B-C''). Note that the number of cytoplasmic dots appears to correlate with the strength of the RNAi-induced intestinal phenotype. Scale bar: 50 µm in A, A'', B, B'', C, C'', 25 µm in A', B', C'.

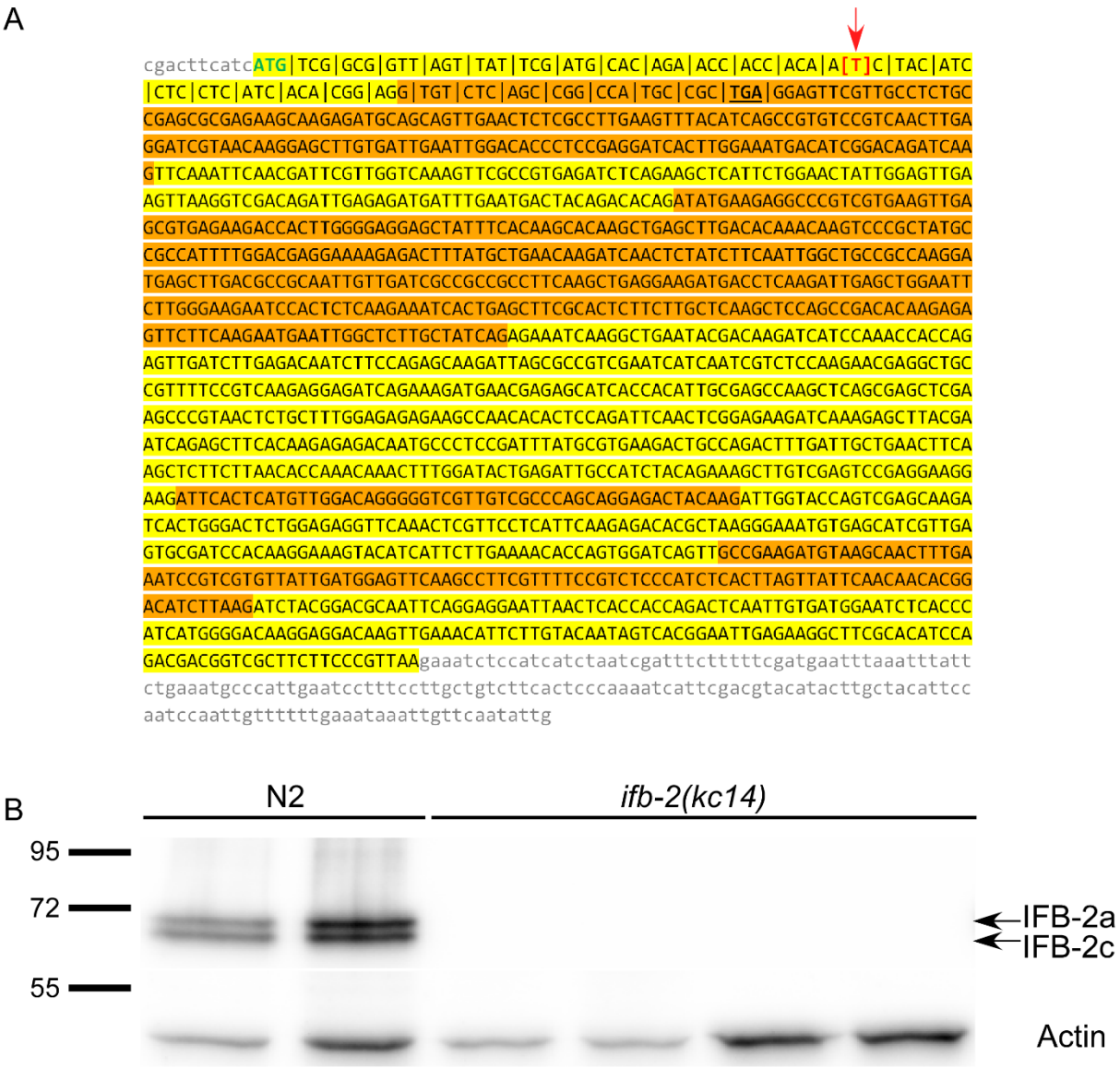

Fig. S4. Genetic alterations of allele *ifb-2(kc14)* and immunoblot analysis of whole worm lysates detecting IFB-2 and actin in N2 and *ifb-2(kc14)*. (A) shows the spliced gene model of *ifb-2* isoform a according to WormBase (www.wormbase.org; exons in alternating colors, non-translated region in grey letters, translational start codon in green). Mutant allele *ifb-2(kc14)* contains a thymidine insertion at position 41 (red arrrow) leading to a premature stop in the second exon (TGA in bold) resulting in a truncated 29 amino acid-long protein encompassing only 13 of the most aminoterminal amino acids of IFB-2a. The mutation also affects all other known IFB-2 isoforms, which share the same start codon and the aminoterminal part encoded by the first five exons. (B) The immunoblot shows complete absence of both IFB-2 isoforms a and c in worms harboring the *ifb-2* knockout allele *kc14*. The blot was subsequently incubated with pan-actin antibodies (lower panel). The position of co-electrophoresed size markers are shown in kDa at left.

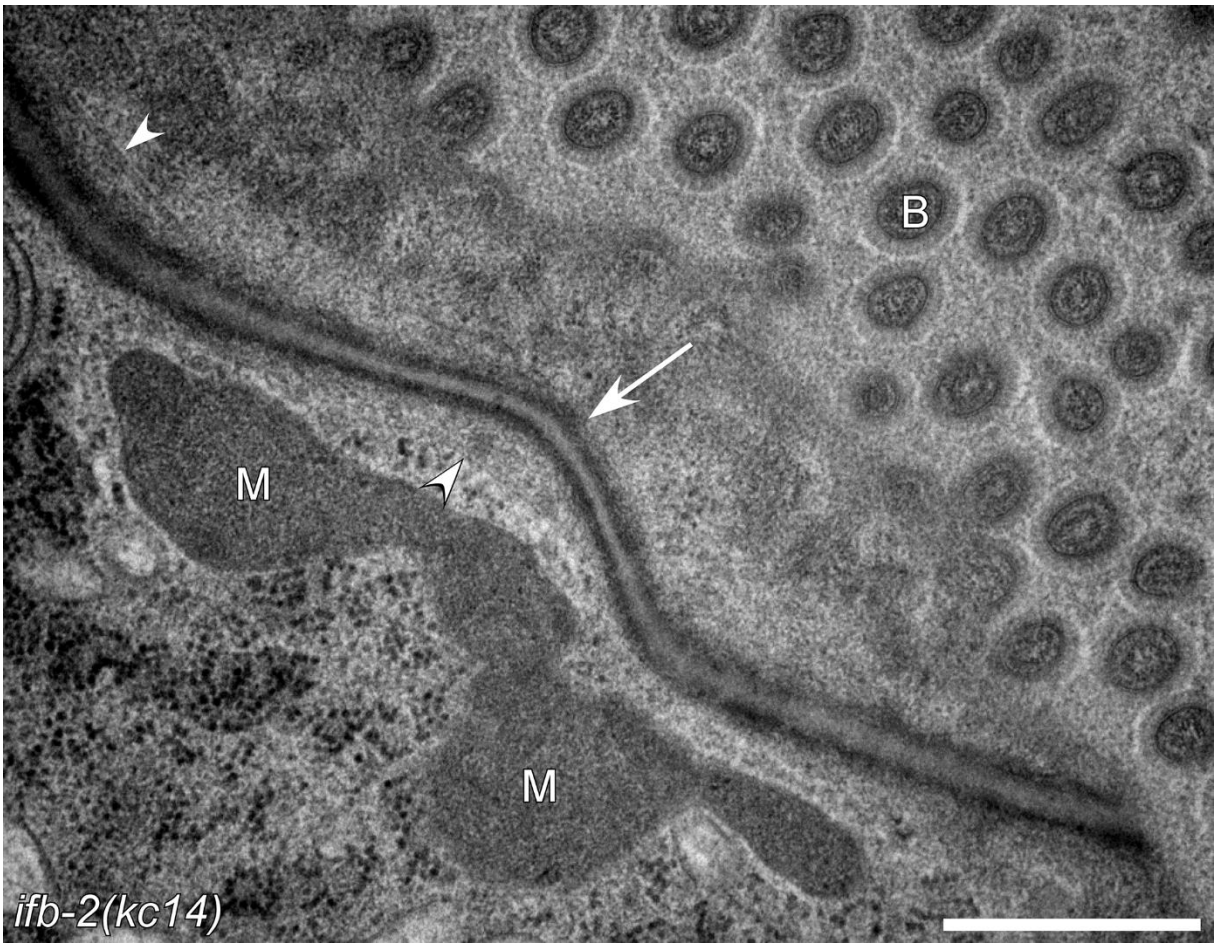

Fig. S5. The *C. elegans* apical junction lacks visible intermediate filaments in IFB-2 knockout animals. The electron micrograph is taken from a young adult *ifb-2(kc14)* knockout animal. The obliquely cut *C. elegans* apical junction appears to be unaffected (white arrow) except for a lack of associated IFs. Note multiple microtubules in close vicinity (white arrowheads). B, brush border; M, mitochondria. Scale bar: 500 nm.

Table S1. List of genes whose expression is either elevated or lowered in isolated intestines of *ifo-1(kc2)*. Transcriptome analyses were performed on intestines dissected from wild-type N2 and *ifo-1(kc2)* L4 mutants. RNA was prepared from 3 separate experiments for gene chip analysis. The list shows 808 upregulated and 256 downregulated genes (fold change >2; p-value <0.05).

Click here to download Table S1

Table S2. List of genes whose expression is either elevated or lowered upon Cry5B treatment in wild-type N2. Transcriptome analyses were performed in animals grown either on control JM103 or on Cry5B-producing JM103 for 4 days. RNA was prepared from 3 separate experiments for gene chip analysis. The list shows 1829 upregulated and 943 downregulated genes (fold change >2; p-value <0.05).

Click here to download Table S2

Table S3. List of genes whose expression is either elevated or lowered upon Cry5B treatment and mutation of the intestinal filament organizer IFO-1. Transcriptome analyses were performed to define similarities/differences of Cry5B intoxication and endotube impairment. RNA was extracted from N2 grown either on control JM103 or on Cry5B-producing JM103 for 4 days and from dissected intestines of adult wild-type and *ifo-1(kc2)*-mutant animals. RNA was extracted from 3 separate pools in each group for gene chip analysis. Comparison of the genes upregulated in both paradigms or downregulated in both paradigms identified 323 candidates (fold change >2; p-value <0.05).

Click here to download Table S3

Table S4. Ontology analysis of genes whose expression is either elevated or lowered by Cry5B treatment and by mutation of the intestinal filament organizer IFO-1. 54 genes are related to the innate immune response and 11 genes to the defense response to Gram-negative bacteria. Membrane rafts and extracellular space were the most affected cellular compartments, and carbohydrate binding was the most altered metabolic function.

Click here to download Table S4